Published in final edited form as:
Matrix Biol. 2010 June ; 29(5): 427–438. doi:10.1016/j.matbio.2010.02.003.

Adult equine bone-marrow stromal cells produce a cartilage-like ECM mechanically superior to animal-matched adult chondrocytes

PW Kopesky[a], **H.-Y. Lee**[b], **EJ Vanderploeg**[a], **JD Kisiday**[d], **DD Frisbie**[d], **AHK Plaas**[e], **C Ortiz**[c], and **AJ Grodzinsky**[a,b]

[a] Massachusetts Institute of Technology Department of Biological Engineering, 77 Massachusetts Avenue Cambridge, MA, 02139

[b] Massachusetts Institute of Technology Department of Electrical Engineering, 77 Massachusetts Avenue Cambridge, MA, 02139

[c] Massachusetts Institute of Technology Department of Materials Science and Engineering 77 Massachusetts Avenue Cambridge, MA, 02139

[d]Colorado State University Department of Clinical Sciences 300 W. Drake Rd. Fort Collins, Colorado 80523

[e]Rush University Medical Center 1735 W. Harrison St. Cohn Research Building Chicago, IL 60612

Abstract

Our objective was to evaluate the age-dependent mechanical phenotype of bone marrow stromal cell-(BMSC-) and chondrocyte-produced cartilage-like neotissue and to elucidate the matrix-associated mechanisms which generate this phenotype. Cells from both immature (2-4 month-old foals) and skeletally-mature (2-5 year-old adults) mixed-breed horses were isolated from animal-matched bone marrow and cartilage tissue, encapsulated in self-assembling-peptide hydrogels, and cultured with and without TGF-β1 supplementation. BMSCs and chondrocytes from both donor ages were encapsulated with high viability. BMSCs from both ages produced neo-tissue with higher mechanical stiffness than that produced by either young or adult chondrocytes. Young, but not adult, chondrocytes proliferated in response to TGF-β1 while BMSCs from both age groups proliferated with TGF-β1. Young chondrocytes stimulated by TGF-β1 accumulated ECM with 10-fold higher sulfated-glycosaminoglycan content than adult chondrocytes and 2-3-fold higher than BMSCs of either age. The opposite trend was observed for hydroxyproline content, with BMSCs accumulating 2-3-fold more than chondrocytes, independent of age. Size-exclusion chromatography of extracted proteoglycans showed that an aggrecan-like peak was the predominant sulfated proteoglycan for all cell types. Direct measurement of aggrecan core protein length and chondroitin sulfate chain length by single molecule atomic force microscopy imaging revealed that, independent of age, BMSCs produced longer core protein and longer chondroitin sulfate chains, and fewer short core protein molecules than chondrocytes, suggesting that the BMSC-produced aggrecan has a phenotype more

Corresponding author: Alan J. Grodzinsky Department of Biological Engineering and MIT Center for Biomedical Engineering Massachusetts Institute of Technology 77 Massachusetts Ave, Rm. NE47-377 Cambridge, MA 02139 phone: 617-253-4969 fax: 617-258-5239 alg@mit.edu.

characteristic of young tissue than chondrocyte-produced aggrecan. Aggrecan ultrastructure, ECM composition, and cellular proliferation combine to suggest a mechanism by which BMSCs produce a superior cartilage-like neotissue than either young or adult chondrocytes.

1. Introduction

Because of their capacity to undergo chondrogenesis (Barry et al. 2001, Johnstone et al. 1998, Pittenger et al. 1999), bone-marrow derived stromal cells (BMSCs) have been the focus of numerous studies with the ultimate goal of repairing cartilage tissue damaged through disease or injury (Connelly et al. 2008, Kisiday et al. 2008, Mauck et al. 2006). Recent reports have suggested a robust chondrogenic and tissue forming capacity for BMSCs that is sustained with aging (Connelly, et al. 2008, Im et al. 2006, Jiang et al. 2008, Scharstuhl et al. 2007), in contrast with primary chondrocytes which have decreased matrix synthesis and tissue repair potential with age (Barbero et al. 2004, Bolton et al. 1999, Plaas and Sandy 1984, Tran-Khanh et al. 2005). This age-related behavior is particularly important given the potential advantages of using autologous tissue for cartilage repair (Chen and Tuan 2008, Noth et al. 2008) making BMSCs an attractive candidate cell source.

Several recent studies have focused on encapsulation of BMSCs in 3D hydrogel culture with TGF-β1 or TGF-β3 stimulation to induce chondrogenesis and compared the differentiated cell phenotype with that of primary chondrocytes (Connelly, et al. 2008, Erickson et al. 2009, Mauck, et al. 2006). While these studies showed that chondrocytes produce a more cartilage-like and mechanically-functional extracellular matrix (ECM) than BMSCs, they all used skeletally-immature bovine tissue as the source for both cell types. Given that the relative chondrogenic potential of chondrocytes vs. BMSCs changes with age, evaluation of chondrocyte- and BMSC-seeded hydrogels at multiple times during development and aging is important.

To achieve cartilage repair, a successful cell-based strategy will be required to recapitulate the fine structure of the native cartilage ECM in order to produce a mechanically functional tissue. Aggrecan, a large aggregating proteoglycan, is the primary cartilage ECM molecule that provides the compressive stiffness and load distribution functions of the tissue (Dudhia 2005). Given the extensive changes in aggrecan biosynthesis (Kimura et al. 1981, Mitchell and Hardingham 1982), processing (Buckwalter et al. 1994, Roughley and White 1980), aggregation (Bolton, et al. 1999) and degradation (Dudhia 2005) with age, it will likely be important to evaluate the quality of aggrecan produced by any cell type used in a cartilage repair therapy. Numerous techniques exist for the study of aggrecan including chromatography (Hascall et al. 1994) and Western analysis (Patwari et al. 2000), which assess size distribution and cleavage products in an entire population of molecules, and imaging techniques such as electron microscopy (Buckwalter and Rosenberg 1982) and atomic force microscopy (AFM; Ng et al. 2003), which allow for detailed measurements of individual molecules.

In this study, we hypothesized that adult BMSCs could produce mechanically-functional cartilage-like neo-tissue comparable to that of primary chondrocytes derived from animal-matched donors. Furthermore we hypothesized that neo-tissue quality for BMSC vs. chondrocyte cell sources would depend on the age of the animal donor. To test these hypotheses, equine bone marrow and cartilage tissue were both harvested from immature foal and skeletally-mature young-adult horses. BMSCs and chondrocytes were isolated and encapsulated in a self-assembling peptide hydrogel that has been shown to enhance TGF-β1 stimulated chondrogenesis of BMSCs and promote accumulation of an aggrecan and type II collagen rich neo-ECM (Kisiday, et al. 2008, Kopesky et al. 2009). These peptides are being developed for use in cardiovascular (Davis et al. 2006, Hsieh et al. 2006), liver (Semino et al.

2003), and cartilage (Kisiday et al. 2002) repair, and have been successfully used in animal studies without inducing inflammation or immune response (Davis, et al. 2006, Hsieh, et al. 2006), making them candidate *in vivo* tissue engineering scaffolds.

Using dynamic compression testing, we measured the neotissue mechanical phenotype produced by BMSCs and chondrocytes from both young and adult animal sources after 21 days of culture. To understand the mechanisms which generate this mechanical phenotype, we quantitatively measured cellular content and ECM synthesis and accumulation. To further assess the quality of the ECM, proteoglycans were extracted and characterized by size exclusion chromatography to examine the size distribution of proteoglycan monomers. Proteoglycan extracts were also purified and imaged by single molecule atomic force microscopy to enable detailed ultrastructural studies of individual aggrecan molecules.

2. Results

2.1 Cell Viability

Both BMSCs and chondrocytes from foal and adult donors survived seeding in peptide hydrogels and were >70% viable one day post-encapsulation in the presence of TGF-β1 (Fig. 1). Similar viability was observed at day 1 in TGF-β1-free controls; however, by day 21, viability in TGF-β1-free controls decreased to 40%-50% for both cell types and both donor ages (not shown), consistent with previous studies (Mouw et al. 2007).

2.2 Mechanical Properties

Both frequency and culture condition were significant main effects on dynamic stiffness (Fig. 2, $p<0.001$), and post-hoc pairwise comparisons on each main effect revealed significant differences between individual frequencies and between different culture conditions. Dynamic stiffness increased monotonically with frequency such that stiffness was 29% higher at 5 Hz than at 0.05 Hz ($p<0.001$). Both adult chondrocyte conditions (with and without TGF-β1) were not significantly different than no cell control hydrogels, while foal BMSCs and chondrocytes in control medium were 50%-60% higher than corresponding frequencies in the no cell controls ($p<0.001$). Foal chondrocytes with TGF-β1 had nearly 4-fold higher dynamic stiffness than no cell controls ($p<0.001$) and 2.5-fold higher stiffness than foal chondrocytes in control medium ($p<0.001$). Both foal and adult BMSCs with TGF-β1 supplementation produced neo-tissue with the highest dynamic stiffness, ~2-fold higher than the foal chondrocytes with TGF-β1 ($p<0.05$), and were not statistically different from each other.

2.3 DNA Content

No significant differences in DNA content were seen between days 0 and 21 for the TGF-β1-free controls suggesting minimal proliferation under these conditions (Fig. 3, note day 0 DNA content not available for adult BMSCs). In contrast, in the presence of TGF-β1, BMSC-seeded hydrogels from both foal and adult donors at day 21 had approximately 2.5-fold higher DNA content than TGF-β1-free (day 21) controls ($p<0.001$). In addition, chondrocytes from foal donors also proliferated in response to TGF-β1, but to a slightly lesser degree than BMSCs, with a 1.6-fold increase in DNA vs. TGF-β1-free controls ($p<0.001$). Chondrocytes isolated from adult donors, however, did not proliferate in response to TGF-β1, suggesting a phenotypic distinction (Fig. 3).

2.4 ECM Content and Biosynthesis

As expected (Tran-Khanh, et al. 2005), foal chondrocyte-seeded peptide hydrogels accumulated significantly higher sGAG per gel than adult chondrocytes both with and without TGF-β1. In the absence of TGF-β1, sGAG accumulation per gel was 7-fold higher for foal

than for adult chondrocytes (Fig. 4A, $p<0.001$), and with TGF-β1 supplementation, sGAG was more than 10-fold higher for the foal compared to adult chondrocyte cultures ($p<0.001$). Minimal sGAG was produced by BMSCs without TGF-β1 stimulation. However, with TGF-β1 supplementation, foal and adult BMSCs accumulated 3-fold and 6-fold higher sGAG than adult chondrocytes, respectively ($p<0.001$). While these day 21 sGAG contents for foal and adult BMSCs were a factor of 2-3 lower than foal chondrocyte sGAG accumulation, when normalized to wet weight, adult BMSC sGAG was not statistically different than foal chondrocyte (Fig. 4B). This effect is due to compaction (defined as the difference between initial and final wet weight divided by the initial wet weight) of the peptide hydrogels by BMSCs but not chondrocytes (data not shown) consistent with our previous studies (Kopesky, et al. 2009).

Consistent with the sGAG content per gel, foal chondrocyte-seeded peptide hydrogels had higher per-cell proteoglycan biosynthesis rates than adult chondrocyte hydrogels during the final day of culture (Fig. 4C, measured by ^{35}S-sulfate incorporation normalized to DNA content), although there was only a 2-fold difference between foal and adult chondrocytes, both with and without TGF-β1 ($p<0.01$). Proteoglycan biosynthesis in BMSC-seeded peptide hydrogels was minimal without TGF-β1 stimulation, but approached the level of foal chondrocytes in the presence of TGF-β1 with foal BMSC cultures only a factor of 2 lower ($p<0.001$) and adult BMSC statistically equivalent to foal chondrocyte hydrogels.

In the presence of TGF-β1, the fraction of sGAG retained vs. the total amount produced (retained plus lost to the medium) was highest for foal chondrocytes at 76% (Fig. 4D), but both foal and adult BMSCs were only 10-20% lower (56% and 66%, respectively, $p<0.001$). In contrast, adult chondrocytes retained only 20% of the sGAG produced, nearly a factor of 4 less than the foal chondrocytes ($p<0.001$).

The hydroxyproline content of the chondrocyte-seeded peptide hydrogels showed similar but less pronounced trends compared to sGAG content. Foal chondrocytes accumulated 10% and 50% higher hydroxyproline per gel than adult chondrocytes, without and with TGF-β1, respectively (Fig. 4E, $p<0.001$). In contrast to sGAG, hydroxyproline content in adult chondrocyte hydrogels did not increase with TGF-β1 stimulation. Also in contrast to sGAG, BMSC-seeded peptide hydrogels had higher hydroxyproline content than chondrocyte-seeded hydrogels. Without TGF-β1, both foal and adult BMSC cultures had 30-40% higher hydroxyproline content per gel than either foal or adult chondrocytes ($p<0.001$). With TGF-β1 supplementation, hydroxyproline content of BMSC cultures was approximately a factor of 2 higher than foal and a factor of 3 higher than adult chondrocytes ($p<0.001$). These effects were even larger when normalized by wet weight, with BMSC cultures ~3-fold higher than foal and ~5-fold higher than adult chondrocytes with TGF-β1 stimulation (Fig. 4F, $p<0.001$).

Protein synthesis rates per cell during the final day of culture (measured by ^{3}H-proline incorporation, Fig. 4G) were largely consistent with total hydroxyproline content. TGF-β1 stimulation produced 2- and 3-fold higher protein synthesis for foal and adult BMSC-seeded cultures than for chondrocyte-seeded peptide hydrogels, respectively ($p<0.01$) with statistically comparable protein synthesis for foal and adult cultures of both cell types. In TGF-β1-free cultures the only significant difference was a lower synthesis rate in adult BMSC hydrogels by a factor of ~4 vs. the other cell types ($p<0.001$).

The ratio of dry weight to wet weight (percentage solid content) was higher for BMSC- than for chondrocyte-seeded peptide hydrogels, indicating greater total matrix density (Fig. 4H). In TGF-β1-free cultures, there was no significant difference between foal and adult chondrocytes (at approximately 1% solid), while foal and adult BMSCs were 20% and 80% higher, respectively (1.2% and 1.8%, $p<0.05$). Foal chondrocytes produced hydrogels that were nearly

2% solid with TGF-β1 stimulation, ~2-fold higher than adult chondrocytes ($p<0.001$). BMSCs were 2-3 fold higher still ($p<0.001$), at 4% and 6% solid for foal and adult BMSCs, respectively. This greater matrix density observed for BMSC than for chondrocyte cultures in the presence of TGF-β1 resulted from both higher dry weight due to matrix accumulation as well as lower wet weight due to BMSC-mediated hydrogel compaction.

2.5 Proteoglycan Size-Exclusion Superose 6 Chromatography

The majority of proteoglycans synthesized in all samples eluted as an aggrecan-like peak (Hascall, et al. 1994) similar to proteoglycans extracted from young bovine cartilage tissue (Fig. 5). Both foal BMSCs and chondrocytes also produced a low, broad peak, to the right of the aggrecan peak, that returned to baseline levels by $K_{av}=0.3$, suggesting a population of smaller proteoglycans was present in these samples (Hascall, et al. 1994). All proteoglycans produced by adult BMSCs and chondrocytes eluted with a K_{av} less than 0.2, suggesting that these samples contained fewer small proteoglycans than the foal cells and were more similar to the native cartilage tissue extract.

2.6 Aggrecan Monomer Ultrastructure via AFM Single Molecule Imaging

Purified proteoglycan extracts from BMSCs and chondrocytes of both animal ages showed individual molecules that displayed a central core and numerous side chains (Fig. 6), consistent with the known core protein-sGAG brush structure of aggrecan as previously visualized by AFM (Ng, et al. 2003). In some cases globular domains were visible on both ends of the core protein, consistent with full-length aggrecan having both G1- and G3-globular domains, while in other cases the sGAG chains may have obscured the G3-domain. Quantitative image analysis revealed that BMSCs from both foals and adults produced aggrecan with significantly longer average core protein length than chondrocytes, 487-503 nm vs. 412-437 nm, respectively (Fig. 7A, $p<0.05$). Further analysis of the distribution of core protein length for all cell types (Fig. 7B) revealed a peak between 500-600 nm, likely representing full-length aggrecan, and a tail that extended below 200 nm, likely due to catabolic processing of the aggrecan core protein. The aggrecan core protein distributions in Fig. 7B showed longer core protein for BMSC samples (26%-29% of aggrecan was >600 nm) than for chondrocyte samples (only 4%-10% of aggrecan is >600 nm). Furthermore, 59%-60% of aggrecan core protein was <500 nm in length for chondrocytes compared with only 31%-36% for BMSCs from either age donor, suggesting a potential increase in aggrecan cleavage in chondrocyte-seeded hydrogels.

High magnification images of single aggrecan monomers had sufficient resolution to clearly distinguish and enable measurement of the lengths of individual CS-GAG chains as previously described (Ng, et al. 2003; example CS-GAGs highlighted in blue on Fig. 6C,F,I,L). CS-GAG chains on BMSC produced aggrecan were longer than on chondrocyte produced aggrecan for both foal cells (Fig. 6E,F vs. 6B,C) and adult cells (Fig. 6K,L vs. 6H,I). Image quantification confirmed this trend with BMSCs from both foals and adults producing 63-73 nm CS-GAG chains while chondrocytes produced CS-GAG chains between 40-46 nm (Fig. 8A, $p<0.05$). To further quantify CS-GAG chain variability within a single aggrecan monomer, the distributions of CS-GAG chain lengths on a single monomer were measured. The examples shown in Fig. 8B represent single monomers each displaying an average CS-GAG length near the population average of Fig. 8A. The distributions for BMSC-produced CS-GAG from both animal ages had higher standard deviation (11-14 nm) than for chondrocyte produced CS-GAG (7-8nm).

3. Discussion

In this study we compared the cartilage-like neo-tissue formed by animal-matched equine BMSCs and chondrocytes as a function of animal donor age. Cells were encapsulated in a self-

assembling peptide hydrogel and both tissue-level measurements to characterize matrix production and mechanical function and single-molecule measurements of ECM extracted aggrecan were made. Chondrogenesis was found to depend on the age of the equine tissue donor from which the cells were derived. For a skeletally-mature adult tissue source, BMSCs produced more sGAG and collagen and assembled a mechanically functional ECM with higher dynamic stiffness than that of primary chondrocytes. In addition, adult BMSCs proliferated during 3D peptide hydrogel culture in response to TGF-β1 stimulation, while adult primary chondrocytes did not. In contrast, BMSCs and chondrocytes from young tissue were both capable of proliferating and producing a mechanically functional tissue in 3D peptide hydrogel culture in the presence of TGF-β1. In the absence of TGF-β1, young primary chondrocytes demonstrated sGAG accumulation and proteoglycan synthesis that was greater than any other cell type in this study yet did not generate a tissue with more than an incremental increase in mechanical properties over cell-free controls. Given both the increases in DNA content per gel disk and the elevated DNA-normalized proteoglycan and protein biosynthesis rates with TGF-β1 supplementation, the higher sGAG and hydroxyproline content of TGF-β1 stimulated neotissue was likely due to a combination of both cell proliferation and increased biosynthesis per cell.

The conclusion that young BMSCs are capable of producing a comparable cartilage-like ECM to young chondrocytes is in contrast to several recent reports using agarose gel culture, including studies by Mauck, et al. 2006, Erickson, et al. 2009, and Connelly, et al. 2008 which showed inferior tissue forming capacity for BMSCs. However, these conclusions were predominantly based on culture in agarose hydrogels, whereas the present study utilized a self-assembling peptide hydrogel, which is known to enhance chondrogenesis of BMSCs relative to agarose (Kopesky, et al. 2009). When peptide hydrogels were used by Erickson, et al. 2009, close agreement with our results was reported at corresponding times in culture for both neo-tissue ECM content and dynamic mechanical stiffness.

Young equine chondrocytes proliferated in response to TGF-β1, whereas adult equine chondrocytes did not (Fig. 3). Peptide gels seeded with young chondrocytes had higher sGAG accumulation and proteoglycan synthesis than adult chondrocytes both with and without TGF-β1 stimulation (Fig. 4A & 4C). This is consistent with a recent report of decreased cellular proliferation and sGAG accumulation by human chondrocytes with age in pellet culture with TGF-β1 stimulation (Barbero, et al. 2004). In addition, when Tran-Khanh, et al. 2005 encapsulated bovine chondrocytes from fetal, young, and aged donors in agarose, a decrease in cell proliferation and sGAG per cell was observed with age. However, Tran-Khanh, et al. 2005 also reported a significant decrease in hydroxyproline content and protein synthesis per cell with age, which was not consistent with the present study using peptide hydrogels.

The dynamic stiffness of BMSC-seeded hydrogels from both young and adult sources was higher than for young chondrocytes (Fig. 2), despite the higher total sGAG content for young chondrocyte-seeded hydrogels (Fig. 4A). To interpret this result, we note that the observed frequency dependence of the dynamic stiffness is consistent with the known poroelastic behavior that characterizes transient and cyclic deformation in a variety of cell-seeded hydrogels (Buschmann et al. 1992,Elisseeff et al. 2000,Mauck et al. 2000), including the peptide hydrogels used here (Kisiday, et al. 2002). The simplest poroelastic description shows that gel dynamic stiffness is regulated by two intrinsic ECM material properties, the equilibrium modulus and hydraulic permeability, which are related to ECM composition (Buschmann, et al. 1992,Elisseeff, et al. 2000,Lee et al. 1981). While the equilibrium modulus and hydraulic permeability are both dependent on the sGAG content of the neo-tissue, they also depend on the density of the solid matrix (Williamson et al. 2001). Both young and adult BMSCs produced a much denser solid matrix (with TGF-β1, Fig. 4H) with significantly higher collagen concentration (OH-Proline per wet weight, Fig. 4F) and comparable sGAG concentration

(sGAG per wet weight, Fig. 4B) compared to young chondrocytes. In addition, BMSCs, but not chondrocytes, from both age donors compacted the hydrogel cultures further increasing the matrix density. Taken together, the BMSC-seeded hydrogels would be expected to have a lower hydraulic permeability than that of young chondrocytes (Eisenberg and Grodzinsky 1988,Mattern et al. 2008), consistent with a higher dynamic stiffness. In addition, the CS-GAG chain length in both BMSC gels was significantly longer than that on aggrecan from primary chondrocytes, independent of age (Fig. 7B). The presence of longer CS-GAG chains is known to increase the nanomolecular compressive stiffness of aggrecan, as previously measured via AFM (Dean et al. 2006), which may result in increased stiffness of the macroscale construct (Fig. 2).

Size exclusion chromatography of the proteoglycans extracted from developing ECM of BMSC- and chondrocyte-seeded peptide hydrogels revealed that the predominant peak detected ran in the void volume of a Superose 6 column (Fig. 5), consistent with the size of aggrecan (Hascall, et al. 1994). This aggrecan peak was observed from ECM extracts from both young and adult cells. However, for both young BMSCs and chondrocytes an additional minor population of proteoglycans was observed near $K_{av} = 0.2$ consistent with the size of decorin (Hascall, et al. 1994), whereas adult BMSCs and chondrocyte samples did not appear to contain a population of small proteoglycans. Alternatively, this population of smaller PGs could be comprised of enzymatically-cleaved aggrecan monomers; however, the resolution limitations of a Superose 6 column does not permit separating these various cleavage products, and hence more detailed analyses were performed via AFM imaging. Nonetheless the chromatography detected predominantly full-length aggrecan, which was consistent with the histograms of core-protein length observed by AFM imaging (Fig. 7B).

When purified aggrecan extracted from BMSC- and chondrocyte-seeded hydrogels was imaged by tapping-mode AFM, the distribution of aggrecan core protein length for both young and adult donors was similar to reported results for aggrecan extracted from young native cartilage (Fig. 7B; Buckwalter and Rosenberg 1982,Buckwalter, et al. 1994,Roughley and White 1980). Ongoing studies have provided further evidence for the production of a young aggrecan phenotype by adult-BMSCs via fluorescence-assisted carbohydrate electrophoresis analysis of the CS-GAG chains (Lee et al. 2009). These findings of consistent aggrecan ultrastructure as a function of BMSC- and chondrocyte-donor age was in contrast with the reported size variability seen for aggrecan extracted from native cartilage of different ages (Buckwalter and Rosenberg 1982,Buckwalter, et al. 1994). These differences are likely due to the diversity of aggrecan structures in adult articular cartilage, in which aggrecan half-life is known to be ~3.5 years (Dudhia 2005), as compared to the newly synthesized aggrecan in the current study. Due to this long residence time in native adult cartilage, aggrecan is susceptible to sustained catabolic activity (Patwari et al. 2005).

Nonetheless, aggrecan molecules with a range of shortened core protein lengths were observed in this study (Fig. 7B), although differences in prevalence of this shortened aggrecan were mainly between chondrocytes and BMSCs and not related to age. One potential explanation for the differences in aggrecan core protein length is that TGF-β1 stimulation has been shown to increase catabolic processing of aggrecan in chondrocyte-seeded agarose (Wilson et al. 2009). In contrast, aggrecan catabolic activity by BMSCs in TGF-β1 stimulated peptide hydrogels is limited (Kopesky, et al. 2009). Thus, the unique distributions of aggrecan core protein length for BMSCs and chondrocytes may be a result of catabolic processing and influenced greatly by the choice of scaffold, cell-scaffold interactions, and cell-type specific responses to TGF-β1 stimulation.

Another unique feature of BMSC produced aggrecan was the trend for molecules to be substituted with elongated CS-GAG chains, which were 40%-75% longer than those on

articular chondrocyte aggrecan (Fig. 8). These elongated CS-GAG chains may indicate a distinct regulatory pathway for CS-GAG biosynthesis in the newly differentiated BMSC population. GAG production is now understood to be independently regulated by expression and organization of transporters and polymerizing enzymes (Little et al. 2008,Victor et al. 2009). CS-GAG elongation has been shown to be enhanced by PDGF, TGFb1, and thrombin (Little, et al. 2008). This has been attributed to downstream signaling mechanisms that enhance transcription and translation of the CS-GAG synthesizing enzymes (Izumikawa et al. 2008,Izumikawa et al. 2007) and that may also affect spatial organization of these proteins into cell type specific GAGOSOMES (Victor, et al. 2009). This suggests that BMSC- and chondrocyte-specific responses to TGF-β1 stimulation may be responsible, in part, for the observed differences in CS-GAG length. One consequence of these elongated CS-GAG chains on BMSC produced aggrecan is that their high anionic charge density and close packing on the core protein would lead to a higher GAG-GAG repulsive force which can extend the core protein length of individual monomers (Ng, et al. 2003). Consistent with this phenomenon, the histograms in Fig. 7B were shifted towards longer core protein length for BMSC-produced aggrecan.

Adult BMSCs encapsulated in a self-assembling peptide hydrogel with TGF-β1 stimulation demonstrated robust cartilage ECM production that was dramatically superior to animal-matched adult chondrocytes, whereas similarly cultured foal chondrocytes had comparable ECM production to foal BMSCs. The newly secreted ECM was mechanically functional and the matrix biochemical composition was consistent with a poroelastic molecular mechanism for the measured mechanical moduli. Detailed AFM analysis of aggrecan monomers synthesized by BMSCs and chondrocytes revealed longer core-protein length and CS-GAG chain length for BMSCs than for chondrocytes, consistent with a younger phenotype for BMSC-produced neotissue (Bolton, et al. 1999, Buckwalter, et al. 1994, Roughley and White 1980). Taken together, these differences suggest potential advantages for BMSCs over chondrocytes for use in cell-seeded cartilage repair strategies, especially when it is desirable to use autologous cells for treatment of adult patients. Future work on BMSC based therapies will need to develop techniques for maintaining the chondrogenic phenotype established during the early chondrogenesis described in this study, without inducing hypertrophy and terminal differentiation. These techniques could potentially involve modifying the cell culture scaffold with bioactive motifs to control the BMSC differentiation state throughout the course of neo-tissue formation, integration with surrounding native tissue, and return to full mechanical and physiologic function.

4. Materials and Methods

4.1 Materials

KLD12 peptide with the sequence AcN-$(KLDL)_3$-CNH_2 was synthesized by the MIT Biopolymers Laboratory (Cambridge, MA) using an ABI Model 433A peptide synthesizer with FMOC protection. All other materials were purchased from the suppliers noted below.

4.2 Tissue Harvest

Cartilage tissue was harvested aseptically from the femoropatellar groove, and bone marrow was harvested from the sternum and iliac crest of two immature (2-4 month-old foals) and three skeletally-mature (2-5 year-old adults) mixed-breed horses as described previously (Kisiday, et al. 2008). Horses were euthanized at Colorado State University for reasons unrelated to conditions that would affect either tissue. Bone marrow and cartilage tissue samples were both harvested from each animal and were processed as animal-matched specimens.

4.3 Cell Isolation

Chondrocytes were isolated by sequential pronase (Sigma-Aldrich, St. Louis, MO), collagenase (Roche Applied Science, Indianapolis, IN) digestion as described previously (Ragan et al. 2000). Marrow samples were washed in PBS and fractionated by centrifugation to remove red blood cells. BMSCs were isolated from the remaining nucleated cell pellet by differential adhesion as described previously (Kisiday, et al. 2008). After BMSC colonies reached local confluence, cells were detached with 0.05% trypsin/1mM EDTA (Invitrogen), reseeded at 6×10^3 cells/cm^2, expanded to ~70% confluence, and cryo-preserved in liquid nitrogen. Prior to peptide hydrogel encapsulation, BMSCs were thawed and plated at 6×10^3 cells/cm^2 in low glucose DMEM plus 10% ES-FBS (embryonic stem cell qualified fetal bovine serum, Invitrogen Carlsbad, CA), 10mM HEPES, and PSA (100 U/mL penicillin, 100 μ/mL streptomycin, and 250 ng/mL amphotericin) plus 5 ng/mL bFGF (R&D Systems, Minneapolis, MN). After 3 days, cells were detached with 0.05% trypsin/1mM EDTA at ~3×10^4 cells/cm^2 (passage 1) and reseeded at 6×10^3 cells/cm^2. Over the subsequent 3 days, this expansion was repeated for passage 2 after which cells were detached for encapsulation in peptide hydrogels.

4.4 Hydrogel Encapsulation and Culture

BMSCs and chondrocytes were encapsulated in 0.35% (w/v) KLD12 peptide at a concentration of 10×10^6 cells/mL using acellular agarose casting molds to initiate peptide assembly as described previously (Kopesky, et al. 2009). Hydrogel disks with an initial volume of 50 μL and dimensions of 6.35 mm diameter by 1.57 mm thick, were cultured in high glucose DMEM (Invitrogen) supplemented with 1% ITS+1 (final concentration: 10 μg/ml insulin, 5.5 μg/ml transferrin, 5 ng/ml sodium selenite, 0.5 mg/ml bovine serum albumin, 4.7 μg/ml linoleic acid, Sigma-Aldrich), 0.1 μM dexamethasone (Sigma-Aldrich), 37.5 μg/mL ascorbate-2-phosphate (Wako Chemicals, Richmond, VA), 1% PSA, 10mM HEPES, 400μM L-proline, 1mM sodium pyruvate, and 1% NEAA, with (+TGF) or without (Cntl) 10 ng/mL recombinant human TGF-β1 (R&D Systems) with medium changes every 2-3 days. For all assays except cell viability, hydrogels were cultured for 21 days.

4.5 Cell Viability

One day after encapsulation, selected specimens from each treatment group of cell-seeded-peptide hydrogels were stained with 350 ng/mL ethidium bromide (dead) and 12.5 μg/mL fluorescein diacetate (live) in PBS and imaged with a Nikon Eclipse fluorescent microscope. The total number of live and dead cells from each of three fields were counted for each animal and % viability was calculated as the number of live cells divided by total number of cells (live + dead).

4.6 Mechanical Stiffness

After 21 days of culture, hydrogels were placed in PBS with protease inhibitors (Protease Complete, Roche) and a digital image was captured from which plug cross-sectional area was measured with the Matlab Image Processing Toolbox (The MathWorks, Natick, MA). For each cell type and medium condition, 6-9 hydrogel disks were tested (3 gels per animal × 2-3 animals). The dynamic stiffness of each plug was measured in uniaxial unconfined compression using a Dynastat mechanical spectrometer (IMASS, Hingham, MA) as described (Frank and Grodzinsky 1987). A 15% offset compression was first applied via three sequential 5% ramp-and-hold steps (5% strain applied over 60 seconds, followed by 4-minute hold), followed by a frequency sweep of 0.5% displacement amplitude sinusoidal strains at 0.05, 0.1, 0.3, 0.5, 1.0, and 5.0 Hz. The dynamic compressive stiffness at each frequency was calculated as the ratio of the fundamental amplitudes of stress to strain (Frank and Grodzinsky 1987). Note no mechanical testing data was recorded for adult BMSCs cultured in TGF-β1-free medium.

4.7 DNA Content and ECM Biochemistry

On day 20 of culture, medium was additionally supplemented with 5 μCi/mL of ^{35}S-sulfate and 10 μCi/mL of ^{3}H-proline to measure cellular biosynthesis of proteoglycans and proteins, respectively. At day 21, hydrogels were rinsed 4×30 minutes in PBS with excess unlabeled sulfate and proline to remove free label. Hydrogels were weighed wet, lyophilized, weighed dry, and digested in 250 μg/mL proteinase-K (Roche) overnight at 60°C. Digested samples were assayed for total DNA content by Hoechst dye binding (Kim et al. 1988), retained sulfated glycosaminoglycan (sGAG) content by DMMB dye binding assay (Farndale et al. 1982), hydroxyproline (OH-Proline) content by chloramine T and p-dimethylaminobenzaldehyde reaction (Woessner 1961), and radiolabel incorporation with a liquid scintillation counter (PerkinElmer 1450 MicroBeta TriLux). Conditioned culture medium collected throughout the study was also analyzed for sGAG content by DMMB dye binding.

4.8 Proteoglycan Size-Exclusion Chromatography

For the final 24 hours, another group of hydrogel specimens from each animal was cultured in medium supplemented with 50 μCi/mL of ^{35}S-sulfate. Proteins were extracted from the minced sample with 4M guanidine HCl and 100mM sodium acetate with protease inhibitors (Protease Complete, Roche) for 48 hours at 4°C with agitation (Roughley and White 1980). Extracts were desalted with a Sephadex G-50 column (GE Healthcare Bio-Sciences, Piscataway, NJ), lyophilized and resuspended in 500mM ammonium acetate for separation on a Superose 6 column (GE Healthcare Bio-Sciences). ^{35}S-sulfate labeled proteoglycans were detected via an inline liquid scintillation counter (Packard Radiomatic Series A-500). For native cartilage tissue extracts, 0.5mL fractions were collected and unlabeled proteoglycans were detected via DMMB dye binding.

4.9 Aggrecan Monomer Extraction and AFM Sample Preparation

Proteins were extracted from separate unlabeled, day 21 hydrogel specimens from 3 adult and 2 foal horses with 4M guanidine as above. Extracts were adjusted to a density of 1.58 g/mL by the addition of CsCl and subjected to density gradient centrifugation at 470,000 g_{av} for 72 hours at 4°C. The gradient was fractionated and the 10 resulting fractions were assayed for density by weighing 80 μL aliquots from each fraction and for sGAG content by DMMB dye binding. Fractions were combined according to density with fractions >1.54 g/mL (labeled D1) expected to contain most of the proteoglycan content of the extract (Roughley and White 1980). The D1 fraction was then dialyzed once against 500 volumes of NaCl, and exhaustively against water at 4°C and sGAG content was quantified by DMMB dye binding.

Aggrecan samples for AFM imaging were prepared as described previously (Ng, et al. 2003). Muscovite mica surfaces (SPI Supplies, West Chester, PA, #1804 V-5) were treated with 0.01% 3-amino-propyltriethoxysilane (APTES; Sigma Aldrich) v/v in MilliQ water (18 MΩ · cm resistivity, Purelab Plus UV/UF, US Filter, Lowell, MA). Sixty microliters of APTES solution was deposited onto freshly cleaved mica, incubated for 20–30 min at room temperature in a humidity controlled environment, rinsed gently with MilliQ water. The APTES-modified mica substrate was then incubated for 20-30 min with 50 μL aliquots of the purified aggrecan solution (prepared as described above) which was diluted to 250 μg/ml final sGAG content in MilliQ filtered water, gently rinsed with MilliQ water and air dried. Electrostatic interaction between the APTES-mica and the aggrecan sGAG chains enabled retention of a population of aggrecan despite rinsing (Ng, et al. 2003). A thin layer of absorbed water 2–10 Å thick exists on the mica surface in ambient conditions (Sheiko and Moller 2001) which partially binds to and hydrates the hydrophilic aggrecan, helping to preserve near physiologic conditions.

4.10 AFM imaging

Imaging was performed as described previously (Ng, et al. 2003). A Nanoscope IIIa Multimode AFM (Digital Instruments (DI), Santa Barbara, CA) was used to image all samples via the EV or JV scanners. Tapping mode was employed in ambient temperature and humidity conditions using Olympus AC240TS-2 rectangular Si cantilevers (k = 2 N/m). The cantilever was driven just below resonant frequency, ω_0, and a slow scan rate of 0.5-1 Hz was used to minimize sample disturbances giving a scan rate that was much slower (<25,000×) than the tap rate. The scans were tested for typical AFM imaging artifacts by varying scan direction, scan size, and rotating the sample. The AFM height images were digitized into pixels, and the aggrecan structural features were traced automatically with a custom Matlab program or manually with SigmaScan Pro image analysis software (SPSS Science, Chicago, IL). The aggrecan core protein length and chondroitin sulfate GAG (CS-GAG) chain length were each measured using the spatial coordinates of the traces. 10–20 AFM images, 2μm × 2μm in size were taken at different locations on the substrate of multiple samples for analysis. In each image, all completely scanned molecules were measured for the core protein length (3–15 aggrecan per image, total number of measured molecules, n = 100–200). About 30 randomly-selected aggrecan molecules from each group was analyzed for the GAG chain length (number of measured, non-intersecting GAG chains per aggrecan = 30–60).

4.11 Statistical Analysis

All data are presented as mean ± sem. Data were analyzed using a mixed model of variance with animal as a random factor. DNA and ECM data were analyzed with a 3-factor model (donor age, cell type, TGF-β1 condition) with 4 repeated measurements for each donor animal, dynamic stiffness data were analyzed with a 2-factor model (frequency and culture condition) with 3 repeated measurements for each donor animal, and core-protein and CS-GAG AFM data were analyzed with a 2-factor model (donor age and cell type). Residual plots were constructed for dependent variable data to test for normality and data were transformed if necessary to satisfy this assumption. *Post hoc* Tukey tests for significance of pairwise comparisons were performed with a threshold for significance of $p<0.05$.

Acknowledgments

The authors would like to thank Ana Mosquera for her contributions to AFM data collection. This work was funded by Grants from the National Institutes of Health (EB003805 and AR33236) and the National Science Foundation (NSF-NIRT 0403903), a National Institutes of Health Molecular, Cell, and Tissue Biomechanics Training Grant Fellowship (P.W.K.), and an Arthritis Foundation Postdoctoral Fellowship (E.J.V.).

References

Barbero A, Grogan S, Schafer D, Heberer M, Mainil-Varlet P, Martin I. Age related changes in human articular chondrocyte yield, proliferation and post-expansion chondrogenic capacity. Osteoarthritis and Cartilage 2004;12:476–484. [PubMed: 15135144]

Barry F, Boynton RE, Liu B, Murphy JM. Chondrogenic differentiation of mesenchymal stem cells from bone marrow: differentiation-dependent gene expression of matrix components. Exp Cell Res 2001;268:189–200. [PubMed: 11478845]

Bolton MC, Dudhia J, Bayliss MT. Age-related changes in the synthesis of link protein and aggrecan in human articular cartilage: implications for aggregate stability. Biochem J 1999;337(Pt 1):77–82. [PubMed: 9854027]

Buckwalter JA, Rosenberg LC. Electron microscopic studies of cartilage proteoglycans. Direct evidence for the variable length of the chondroitin sulfate-rich region of proteoglycan subunit core protein. J Biol Chem 1982;257:9830–9839. [PubMed: 6809744]

Buckwalter JA, Roughley PJ, Rosenberg LC. Age-related changes in cartilage proteoglycans: quantitative electron microscopic studies. Microsc Res Tech 1994;28:398–408. [PubMed: 7919527]

Buschmann MD, Gluzband YA, Grodzinsky AJ, Kimura JH, Hunziker EB. Chondrocytes in agarose culture synthesize a mechanically functional extracellular matrix. J Orthop Res 1992;10:745–758. [PubMed: 1403287]

Calabro A, Midura R, Wang A, West L, Plaas A, Hascall VC. Fluorophore-assisted carbohydrate electrophoresis (FACE) of glycosaminoglycans. Osteoarthritis Cartilage 2001;9(Suppl A):S16–22. [PubMed: 11680680]

Chen FH, Tuan RS. Mesenchymal stem cells in arthritic diseases. Arthritis Res Ther 2008;10:223. [PubMed: 18947375]

Connelly JT, Wilson CG, Levenston ME. Characterization of proteoglycan production and processing by chondrocytes and BMSCs in tissue engineered constructs. Osteoarthritis Cartilage 2008;16:1092–1100. [PubMed: 18294870]

Davis ME, Hsieh PC, Takahashi T, Song Q, Zhang S, Kamm RD, Grodzinsky AJ, Anversa P, Lee RT. Local myocardial insulin-like growth factor 1 (IGF-1) delivery with biotinylated peptide nanofibers improves cell therapy for myocardial infarction. Proc Natl Acad Sci U S A 2006;103:8155–8160. [PubMed: 16698918]

Dean D, Han L, Grodzinsky AJ, Ortiz C. Compressive nanomechanics of opposing aggrecan macromolecules. J Biomech 2006;39:2555–2565. [PubMed: 16289077]

Dudhia J. Aggrecan, aging and assembly in articular cartilage. Cell Mol Life Sci 2005;62:2241–2256. [PubMed: 16143826]

Eisenberg SR, Grodzinsky AJ. Electrokinetic micromodel of extracellular matrix and other polyelectrolyte networks. PhysicoChemical Hydrodynamics 1988;10:517–539.

Elisseeff J, McIntosh W, Anseth K, Riley S, Ragan P, Langer R. Photoencapsulation of chondrocytes in poly(ethylene oxide)-based semi-interpenetrating networks. J Biomed Mater Res 2000;51:164–171. [PubMed: 10825215]

Erickson IE, Huang AH, Chung C, Li RT, Burdick JA, Mauck RL. Differential maturation and structure-function relationships in mesenchymal stem cell- and chondrocyte-seeded hydrogels. Tissue Eng Part A 2009;15:1041–1052. [PubMed: 19119920]

Farndale RW, Sayers CA, Barrett AJ. A direct spectrophotometric microassay for sulfated glycosaminoglycans in cartilage cultures. Connect Tissue Res 1982;9:247–248. [PubMed: 6215207]

Frank EH, Grodzinsky AJ. Cartilage electromechanics--I. Electrokinetic transduction and the effects of electrolyte pH and ionic strength. J Biomech 1987;20:615–627. [PubMed: 3611137]

Hascall VC, Calabro A, Midura RJ, Yanagishita M. Isolation and characterization of proteoglycans. Methods Enzymol 1994;230:390–417. [PubMed: 8139509]

Hsieh PC, Davis ME, Gannon J, MacGillivray C, Lee RT. Controlled delivery of PDGF-BB for myocardial protection using injectable self-assembling peptide nanofibers. J Clin Invest 2006;116:237–248. [PubMed: 16357943]

Im GI, Jung NH, Tae SK. Chondrogenic Differentiation of Mesenchymal Stem Cells Isolated from Patients in Late Adulthood: The Optimal Conditions of Growth Factors. Tissue Eng 2006;12:527–537. [PubMed: 16579686]

Izumikawa T, Koike T, Shiozawa S, Sugahara K, Tamura J, Kitagawa H. Identification of chondroitin sulfate glucuronyltransferase as chondroitin synthase-3 involved in chondroitin polymerization: chondroitin polymerization is achieved by multiple enzyme complexes consisting of chondroitin synthase family members. J Biol Chem 2008;283:11396–11406. [PubMed: 18316376]

Izumikawa T, Uyama T, Okuura Y, Sugahara K, Kitagawa H. Involvement of chondroitin sulfate synthase-3 (chondroitin synthase-2) in chondroitin polymerization through its interaction with chondroitin synthase-1 or chondroitin-polymerizing factor. Biochem J 2007;403:545–552. [PubMed: 17253960]

Jiang Y, Mishima H, Sakai S, Liu YK, Ohyabu Y, Uemura T. Gene expression analysis of major lineage-defining factors in human bone marrow cells: effect of aging, gender, and age-related disorders. J Orthop Res 2008;26:910–917. [PubMed: 18302252]

Johnstone B, Hering TM, Caplan AI, Goldberg VM, Yoo JU. In vitro chondrogenesis of bone marrow-derived mesenchymal progenitor cells. Exp Cell Res 1998;238:265–272. [PubMed: 9457080]

Kim YJ, Sah RL, Doong JY, Grodzinsky AJ. Fluorometric assay of DNA in cartilage explants using Hoechst 33258. Anal Biochem 1988;174:168–176. [PubMed: 2464289]

Kimura JH, Caputo CB, Hascall VC. The effect of cycloheximide on synthesis of proteoglycans by cultured chondrocytes from the Swarm rat chondrosarcoma. J Biol Chem 1981;256:4368–4376. [PubMed: 6783661]

Kisiday J, Jin M, Kurz B, Hung H, Semino C, Zhang S, Grodzinsky AJ. Self-assembling peptide hydrogel fosters chondrocyte extracellular matrix production and cell division: implications for cartilage tissue repair. Proc Natl Acad Sci U S A 2002;99:9996–10001. [PubMed: 12119393]

Kisiday JD, Kopesky PW, Evans CH, Grodzinsky AJ, McIlwraith CW, Frisbie DD. Evaluation of adult equine bone marrow- and adipose-derived progenitor cell chondrogenesis in hydrogel cultures. J Orthop Res 2008;26:322–331. [PubMed: 17960654]

Kopesky PW, Vanderploeg EJ, Sandy JD, Kurz B, Grodzinsky AJ. Self-Assembling Peptide Hydrogels Modulate In Vitro Chondrogenesis of Bovine Bone Marrow Stromal Cells Tissue Eng Part A. 2009 (in press).

Lee, H-Y.; Kopesky, PW.; Plaas, AHK.; Diaz, MA.; Sandy, JD.; Frisbie, DD.; Kisiday, JD.; Ortiz, C.; Grodzinsky, AJ. Adult Equine MSCs Synthesize Aggrecan having Nanomechanical Compressibility and Biochemical Composition Characteristic of Young Growth Cartilage. Presented at the 55th Orthopedic Research Society; Las Vegas, NV. February 22-25, 2009; 2009.

Lee RC, Frank EH, Grodzinsky AJ, Roylance DK. Oscillatory compressional behavior of articular cartilage and its associated electromechanical properties. J Biomech Eng 1981;103:280–292. [PubMed: 7311495]

Little PJ, Ballinger ML, Burch ML, Osman N. Biosynthesis of natural and hyperelongated chondroitin sulfate glycosaminoglycans: new insights into an elusive process. Open Biochem J 2008;2:135–142. [PubMed: 19238187]

Mattern KJ, Nakornchai C, Deen WM. Darcy permeability of agarose-glycosaminoglycan gels analyzed using fiber-mixture and donnan models. Biophys J 2008;95:648–656. [PubMed: 18375508]

Mauck RL, Soltz MA, Wang CC, Wong DD, Chao PH, Valhmu WB, Hung CT, Ateshian GA. Functional tissue engineering of articular cartilage through dynamic loading of chondrocyte-seeded agarose gels. J Biomech Eng 2000;122:252–260. [PubMed: 10923293]

Mauck RL, Yuan X, Tuan RS. Chondrogenic differentiation and functional maturation of bovine mesenchymal stem cells in long-term agarose culture. Osteoarthritis Cartilage 2006;14:179–189. [PubMed: 16257243]

Mitchell D, Hardingham T. The control of chondroitin sulphate biosynthesis and its influence on the structure of cartilage proteoglycans. Biochem J 1982;202:387–395. [PubMed: 6807292]

Mouw JK, Connelly JT, Wilson CG, Michael KE, Levenston ME. Dynamic compression regulates the expression and synthesis of chondrocyte-specific matrix molecules in bone marrow stromal cells. Stem Cells 2007;25:655–663. [PubMed: 17124008]

Ng L, Grodzinsky AJ, Patwari P, Sandy J, Plaas A, Ortiz C. Individual cartilage aggrecan macromolecules and their constituent glycosaminoglycans visualized via atomic force microscopy. J Struct Biol 2003;143:242–257. [PubMed: 14572479]

Noth U, Steinert AF, Tuan RS. Technology insight: adult mesenchymal stem cells for osteoarthritis therapy. Nat Clin Pract Rheumatol 2008;4:371–380. [PubMed: 18477997]

Patwari P, Gao G, Lee JH, Grodzinsky AJ, Sandy JD. Analysis of ADAMTS4 and MT4-MMP indicates that both are involved in aggrecanolysis in interleukin-1-treated bovine cartilage. Osteoarthritis Cartilage 2005;13:269–277. [PubMed: 15780640]

Patwari P, Kurz B, Sandy JD, Grodzinsky AJ. Mannosamine inhibits aggrecanase-mediated changes in the physical properties and biochemical composition of articular cartilage. Arch Biochem Biophys 2000;374:79–85. [PubMed: 10640399]

Pittenger MF, Mackay AM, Beck SC, Jaiswal RK, Douglas R, Mosca JD, Moorman MA, Simonetti DW, Craig S, Marshak DR. Multilineage potential of adult human mesenchymal stem cells. Science 1999;284:143–147. [PubMed: 10102814]

Plaas AH, Sandy JD. Age-related decrease in the link-stability of proteoglycan aggregates formed by articular chondrocytes. Biochem J 1984;220:337–340. [PubMed: 6743270]

Ragan PM, Chin VI, Hung HH, Masuda K, Thonar EJ, Arner EC, Grodzinsky AJ, Sandy JD. Chondrocyte extracellular matrix synthesis and turnover are influenced by static compression in a new alginate disk culture system. Arch Biochem Biophys 2000;383:256–264. [PubMed: 11185561]

Roughley PJ, White RJ. Age-related changes in the structure of the proteoglycan subunits from human articular cartilage. J Biol Chem 1980;255:217–224. [PubMed: 7350154]

Scharstuhl A, Schewe B, Benz K, Gaissmaier C, Buhring HJ, Stoop R. Chondrogenic potential of human adult mesenchymal stem cells is independent of age or osteoarthritis etiology. Stem Cells 2007;25:3244–3251. [PubMed: 17872501]

Semino CE, Merok JR, Crane GG, Panagiotakos G, Zhang S. Functional differentiation of hepatocyte-like spheroid structures from putative liver progenitor cells in three-dimensional peptide scaffolds. Differentiation 2003;71:262–270. [PubMed: 12823227]

Sheiko SS, Moller M. Visualization of macromolecules--a first step to manipulation and controlled response. Chem Rev 2001;101:4099–4124. [PubMed: 11740928]

Tran-Khanh N, Hoemann CD, McKee MD, Henderson JE, Buschmann MD. Aged bovine chondrocytes display a diminished capacity to produce a collagen-rich, mechanically functional cartilage extracellular matrix. J Orthop Res 2005;23:1354–1362. [PubMed: 16048738]

Victor XV, Nguyen TK, Ethirajan M, Tran VM, Nguyen KV, Kuberan B. Investigating the elusive mechanism of glycosaminoglycan biosynthesis. J Biol Chem 2009;284:25842–25853. [PubMed: 19628873]

Williamson AK, Chen AC, Sah RL. Compressive properties and function-composition relationships of developing bovine articular cartilage. J Orthop Res 2001;19:1113–1121. [PubMed: 11781013]

Wilson CG, Nishimuta JF, Levenston ME. Chondrocytes and meniscal fibrochondrocytes differentially process aggrecan during de novo extracellular matrix assembly. Tissue Eng Part A 2009;15:1513–1522. [PubMed: 19260779]

Woessner JF Jr. The determination of hydroxyproline in tissue and protein samples containing small proportions of this imino acid. Arch Biochem Biophys 1961;93:440–447. [PubMed: 13786180]

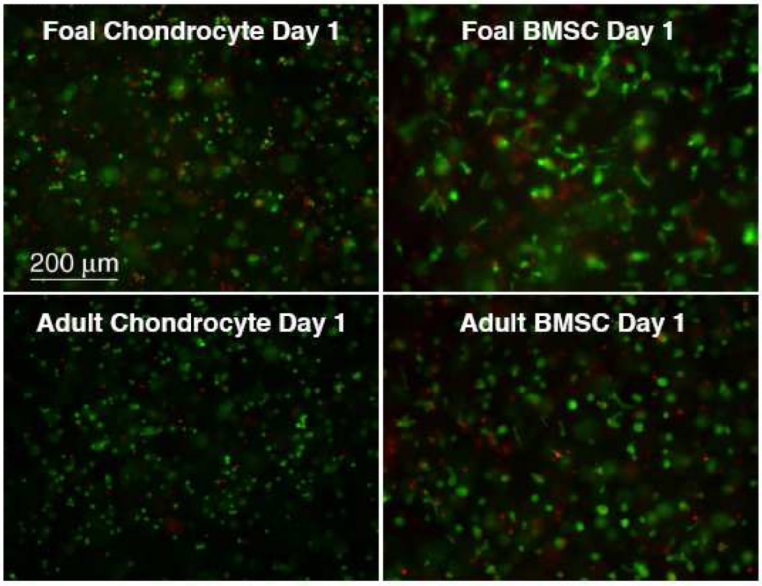

Figure 1.
Cell Viability. Live **(green)** and dead **(red)** staining of self-assembling peptide hydrogels cultured with TGF-β1 at day 1.

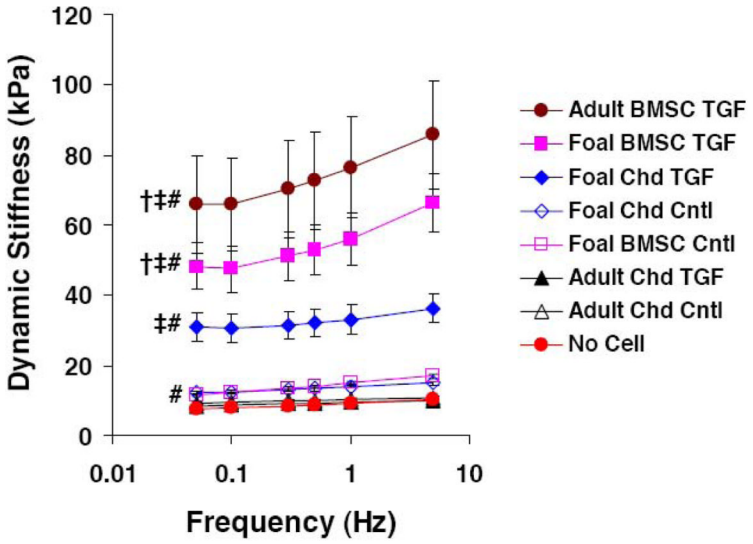

Figure 2.

Hydrogel Dynamic Stiffness. Chondrocyte **(Chd)** and BMSC seeded peptide hydrogels after 21 days of culture in control **(Cntl)** or TGF-β1 supplemented **(TGF)** medium. **Stats:** mean ± sem, n=2 foals × 3 samples each or n=3 adults × 3 samples each; ‡ vs. foal chondrocyte TGF, † vs. foal chondrocyte Cntl, # vs. No Cell; $p<0.05$.

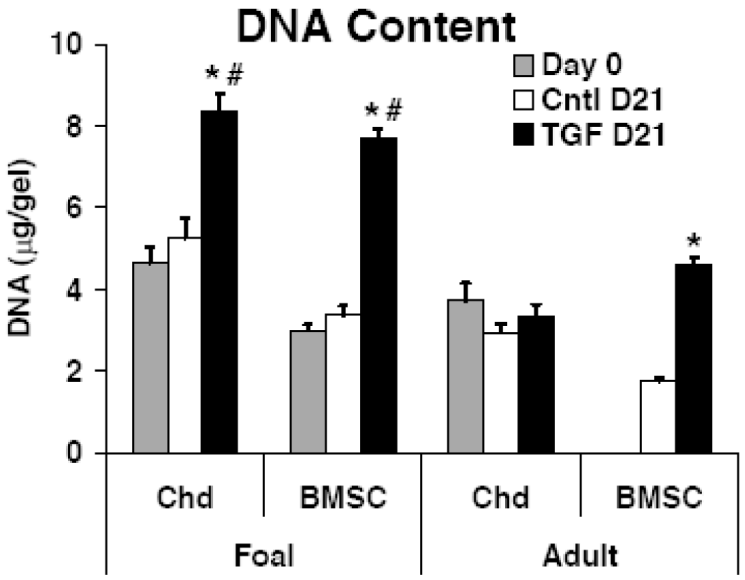

Figure 3.
Hydrogel DNA Content. DNA content for chondrocyte and BMSC hydrogels at day 0, or after 21 days. **Stats:** mean ± sem, n=2 foals × 4 samples each or n=3 adults × 4 samples each; for a given cell type and age significance is indicated by: # vs. Day 0; * vs. Cntl D21; $p<0.001$.

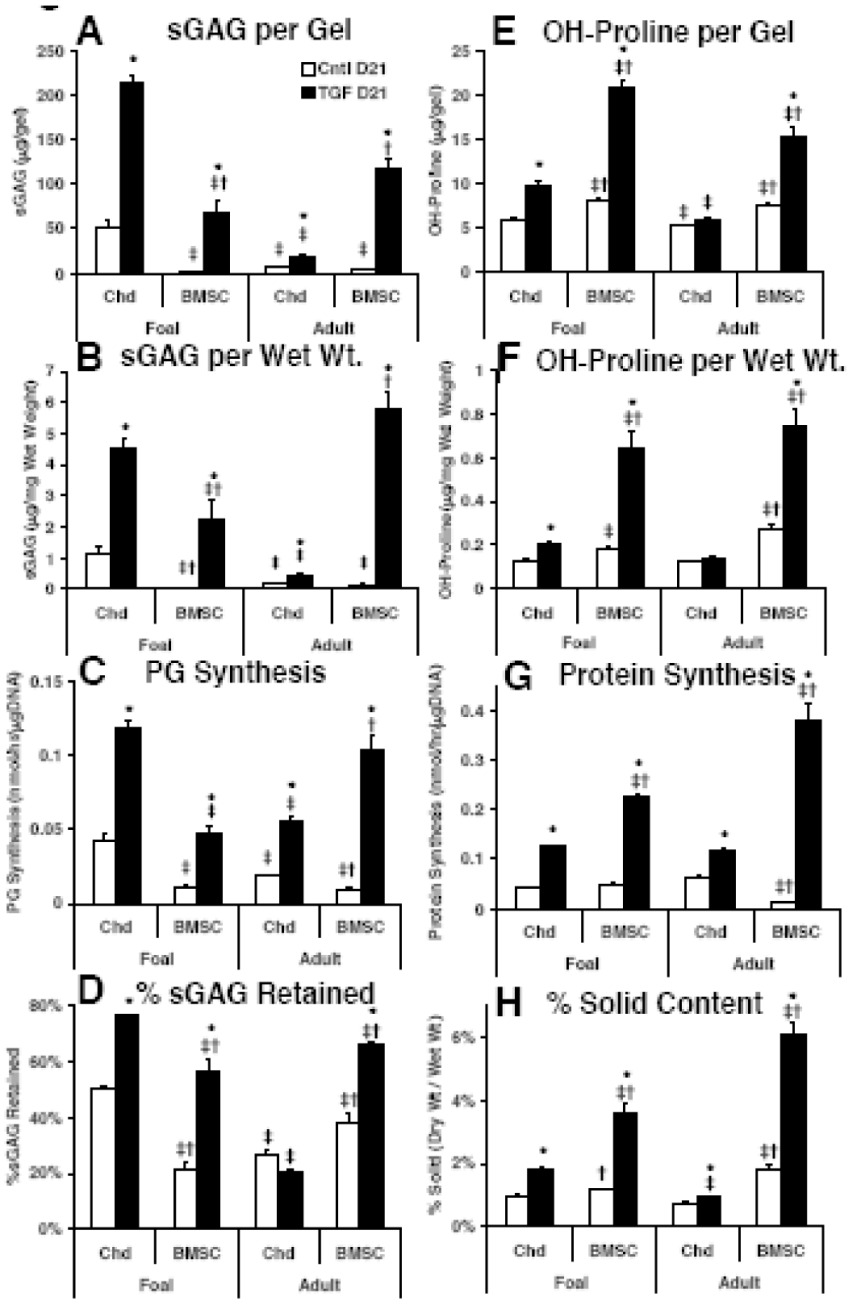

Figure 4.

Hydrogel ECM Content and Biosythesis Rates at Day 21. sGAG content **(A)** per hydrogel **(B)** per wet weight. **(C)** Proteoglycan biosynthesis. **(D)** %sGAG retention. Hydroxyproline content **(E)** per hydrogel **(F)** per wet weight. **(G)** Protein biosynthesis **(H)** %Solid matrix. **Stats:** mean±sem, n=2 foals × 4 samples each or n=3 adults × 4 samples each; * vs. Cntl; ‡ vs. foal chondrocyte; † vs. adult chondrocyte; $p<0.05$.

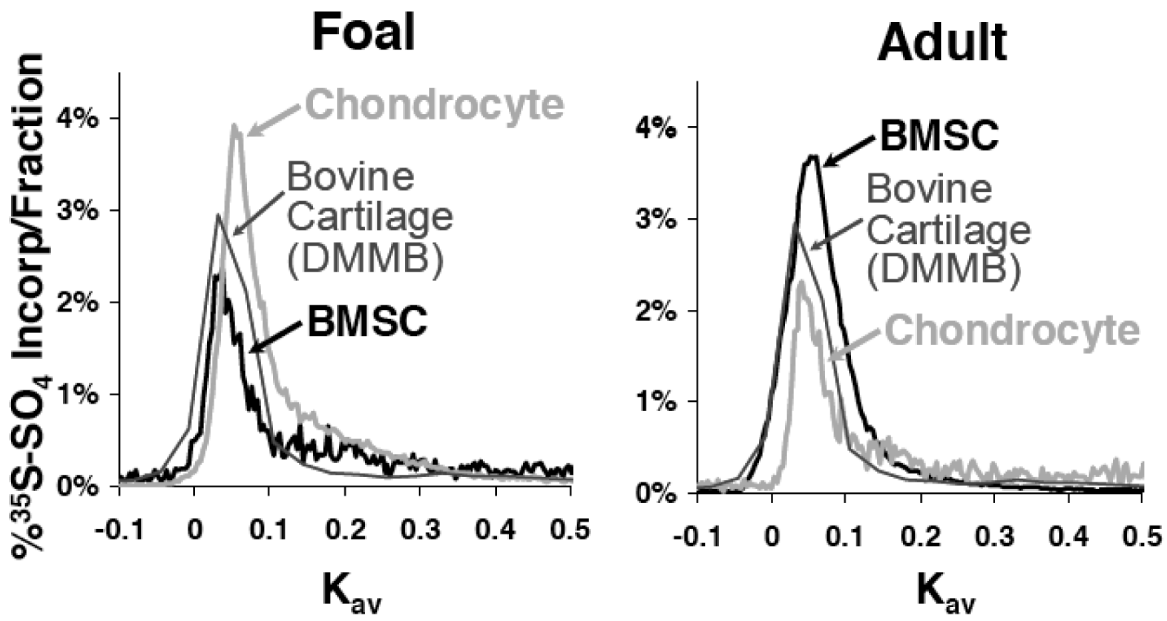

Figure 5.

Superose 6, Size-Exclusion, Proteoglycan Chromatography. Proteoglycans extracted from either chondrocyte and BMSC seeded peptide hydrogels after 21 days of culture with TGF-β1 or from native cartilage tissue harvested from newborn bovine calves.

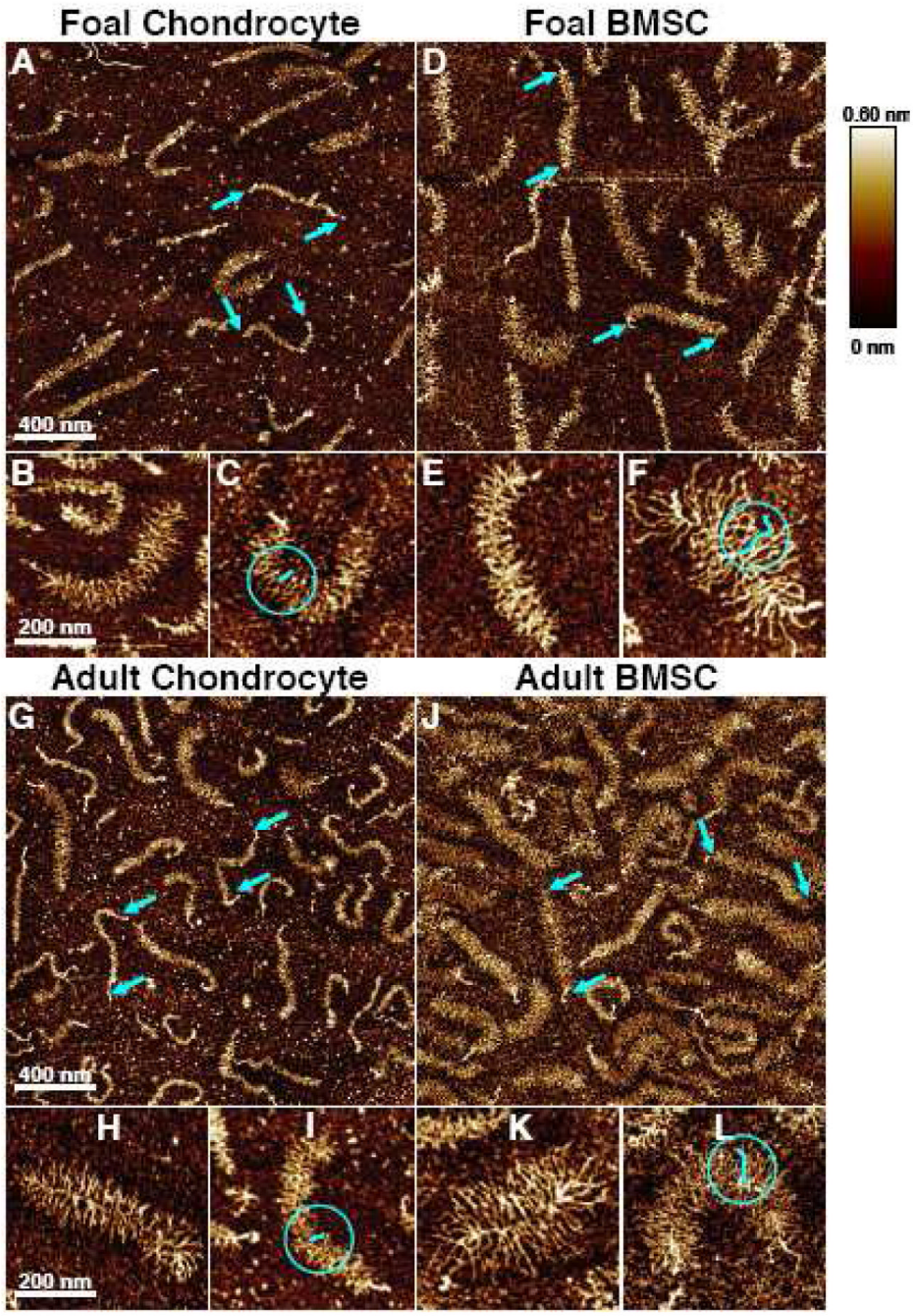

Figure 6.

AFM Single-Molecule Height Images of Aggrecan Ultrastructure. Proteoglycans extracted from cell-seeded peptide hydrogels after 21 days of culture with TGF-β1. **(A-C)** Foal chondrocytes, **(D-F)** Foal BMSCs, **(G-I)** Adult chondrocytes, **(J-L)** Adult BMSCs. Blue arrows in A,D,G,J denote ends of full-length aggrecan monomers. Example individual CS-GAG chains highlighted in blue in C,F,I,L.

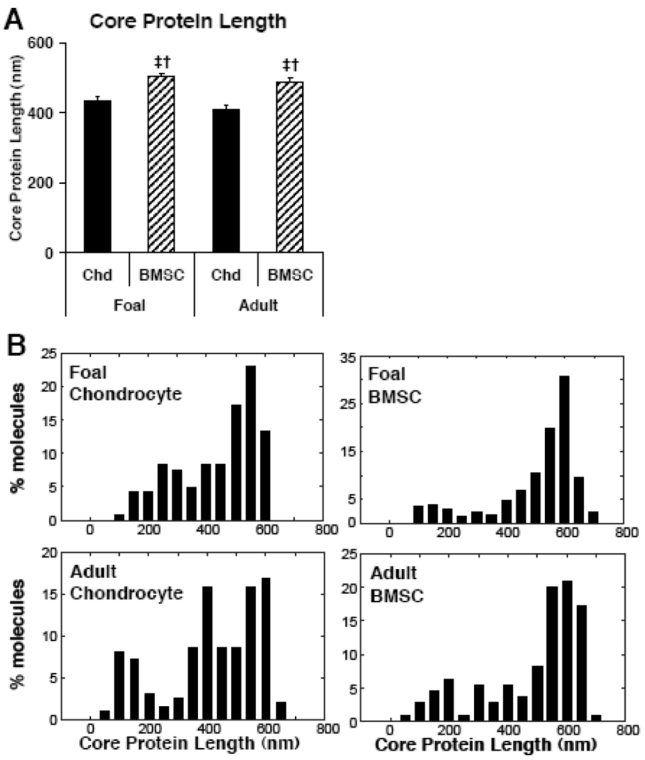

Figure 7.

Aggrecan Core Protein Quantification. Aggrecan extracted from chondrocyte **(Chd)** and BMSC seeded peptide hydrogels after 21 days of culture with TGF-β1. **(A)** Core-protein average length. **Stats:** mean ± sem; n=110-231 aggrecan molecules; ‡ vs. foal chondrocyte; † vs. adult chondrocyte; $p<0.05$. **(B)** Histograms of core-protein length.

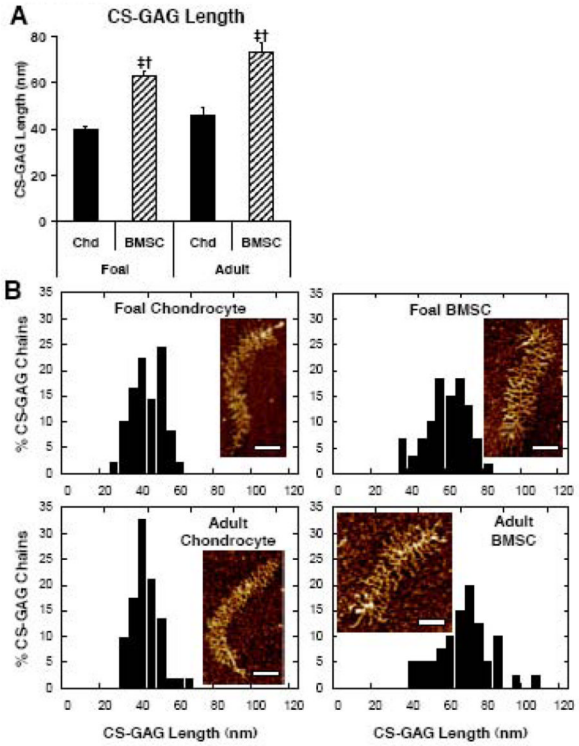

Figure 8.

Aggrecan CS-GAG Chain Quantificaiton. Aggrecan extracted from chondrocyte **(Chd)** and BMSC seeded peptide hydrogels after 21 days of culture with TGF-β1. **(A)** Average CS-GAG length per molecule. **Stats:** mean ± sem; n=28-35 aggrecan molecules; ‡ vs. foal chondrocyte; † vs. adult chondrocyte; $p<0.05$. **(B)** Histograms of CS-GAG distribution on the single pictured molecule. Scale bar = 100 nm.